

DTIC FILE COPY

2

AD-A233 000

OFFICE OF NAVAL RESEARCH

Contract N00014-87-J-1118

R & T Code 4133016

Technical Report No. 19

**The Application of Concentration-Distance Profiling
Raman Microspectroscopy to the Study of the
Photoinduced Crystallization of Triethylenediamine Triiodide
Upon a Silver Electrode**

by

T. Ozeki and D.E. Irish

Prepared for Publication

in

Journal of Physical Chemistry

**DTIC
ELECTE
MAR 15 1991
S B D**

**Guelph-Waterloo Center for Graduate Work in Chemistry
Waterloo Campus
Department of Chemistry
University of Waterloo
Waterloo, Ontario
Canada, N2L 3G1**

February 15, 1991

**Reproduction in whole or in part is permitted for
any purpose of the United States Government**

***This document has been approved for public release
and sale; its distribution is unlimited.**

91 3 11 047

b. DECLASSIFICATION / DOWNGRADING SCHEDULE		Public Release/Unlimited	
4. PERFORMING ORGANIZATION REPORT NUMBER(S) ONR Technical Report #19		5. MONITORING ORGANIZATION REPORT NUMBER(S)	
a. NAME OF PERFORMING ORGANIZATION D. E. Irish University of Waterloo	6b. OFFICE SYMBOL (if applicable)	7a. NAME OF MONITORING ORGANIZATION Office of Naval Research	
c. ADDRESS (City, State, and ZIP Code) Department of Chemistry University of Waterloo Waterloo, Ontario, Canada, N2L 3G1		7b. ADDRESS (City, State, and ZIP Code) The Ohio State University, Research Center 1314 Kinnear Road, Room 318 Columbus, Ohio, U.S.A., 43212-1194	
a. NAME OF FUNDING / SPONSORING ORGANIZATION Office of Naval Research	8b. OFFICE SYMBOL (if applicable)	9. PROCUREMENT INSTRUMENT IDENTIFICATION NUMBER N00014-87-J-1118	
c. ADDRESS (City, State, and ZIP Code) Chemistry Division 800 N. Quincy Street Arlington, VA, U.S.A., 22217-5000		10. SOURCE OF FUNDING NUMBERS	
		PROGRAM ELEMENT NO.	PROJECT NO.
		TASK NO.	WORK UNIT ACCESSION NO.
1. TITLE (Include Security Classification) The Application of Concentration-Distance Profiling Raman Microspectroscopy to the Study of the Photoinduced Crystallization of Triethylenediamine Triiodide Upon a Silver Electrode			
2. PERSONAL AUTHOR(S) T. Ozeki and D.E. Irish			
3a. TYPE OF REPORT Technical	13b. TIME COVERED FROM 08/90 TO 12/90	14. DATE OF REPORT (Year, Month, Day) 1990-02-15	15. PAGE COUNT 18
5. SUPPLEMENTARY NOTATION Submitted to Journal of Physical Chemistry			
7. COSATI CODES		18. SUBJECT TERMS (Continue on reverse if necessary and identify by block number)	
FIELD	GROUP	SUB-GROUP	
		Concentration-distance profiling by Raman microspectroscopy; species concentrations in the diffusion layer; crystalline diprotonated DABCO triiodide	
9. ABSTRACT (Continue on reverse if necessary and identify by block number)			

The technique of concentration-distance profiling Raman microspectroscopy has been applied to the system silver/triethylenediamine, HClO_4 , NaI , H_2O to map out the variations in the concentrations of species with distance from the electrode surface. Under anodic conditions crystals of triethylenediamine triiodide grow from the site of laser illumination. These have also been studied; they extend some 200 μm from the silver electrode surface with maximum population at about 40 μm . Under cathodic conditions the crystals are destroyed and the surface is covered with iodide interacting in an ion-pairing fashion with diprotonated triethylenediamine, abbreviated DABCO-H_2^{2+} .

0. DISTRIBUTION / AVAILABILITY OF ABSTRACT <input checked="" type="checkbox"/> UNCLASSIFIED/UNLIMITED <input type="checkbox"/> SAME AS RPT. <input type="checkbox"/> DTIC USERS		21. ABSTRACT SECURITY CLASSIFICATION Unclassified	
2a. NAME OF RESPONSIBLE INDIVIDUAL Dr. Robert J. Nowak		22b. TELEPHONE (Include Area Code) (519) 885-1211, ext. 2500	22c. OFFICE SYMBOL

**THE APPLICATION OF CONCENTRATION-DISTANCE
PROFILING RAMAN MICROSCOPY TO THE STUDY
OF THE PHOTOINDUCED CRYSTALLIZATION OF
TRIETHYLENEDIAMINE TRIIODIDE UPON A SILVER ELECTRODE**

Toru Ozeki[†] and Donald E. Irish^{*}

^{*}Department of Chemistry
University of Waterloo
Waterloo, Ontario
Canada N2L 3G1

[†]Present Address: Hyogo University of Teacher Education, 942-1
Shimokume, Yashiro-cho
Kato-gun, Hyogo
Japan 673-14

Abstract

The technique of concentration-distance profiling Raman microspectroscopy has been applied to the system silver/triethylenediamine, HClO_4 , NaI , H_2O to map out the variations in the concentrations of species with distance from the electrode surface. Under anodic conditions crystals of triethylenediamine triiodide grow from the site of laser illumination. These have also been studied; they extend some 200 μm from the silver electrode surface with maximum population at about 40 μm . Under cathodic conditions the crystals are destroyed and the surface is covered with iodide interacting in an ion-pairing fashion with diprotonated triethylenediamine, abbreviated DABCO-H_2^{2+} .

Introduction

At potentials anodic of -150 mV, on a silver electrode in the presence of an aqueous solution of 0.1 M DABCO and 0.5 M NaI with a pH of 0.45, adjusted with perchloric acid, and under 514.5 nm laser illumination, crystals of $\text{DABCO-H}_2^{2+} (\text{I}_3^-)_2$ grow from the site of illumination. The mechanism for this photoinduced crystallization together with the supporting spectroscopic and electrochemical evidence are described in the previous paper.¹ Here we report the spatial distribution of the crystals as measured with a new technique - Concentration-Distance Profiling Raman Microspectroscopy or CDPRMS.² This method complements others³ which have been developed to measure the variation in concentration of species in the diffusion layer which lies between the inner layers and the bulk solution adjacent to an electrode surface.

The method has high specificity because the unique vibrational spectra of the different species are measured. Simply described (see ref. 2) the objective lens of a Raman microscope is focussed at different distances, x , between an electrode surface ($x=0$) and the optical window of a spectroelectrochemical cell; for each position a Raman spectrum is recorded. The variation with distance of Raman peak intensities provides a measure of the variation of the concentration of that species with distance. With present technology the distance-steps are 2 μm . Considering the



Codes

and/or
Special

1A-11

normal aperture of the objective and the focal cylinder of the laser beam the spatial resolution is about 10 μm . For the case of the electrolysis of the $\text{Fe}(\text{CN})_6^{3-}/\text{Fe}(\text{CN})_6^{4-}$ couple at a gold electrode, concentration variations in an unstirred cell were observed for $0 < x \leq 200 \mu\text{m}$ from a polished gold electrode surface.² Here we report the application of this technique to the diprotonated DABCO triiodide crystal system.

Experimental

Spectral measurements were made with the Dilor OMARS-89 Raman spectrometer equipped with microscope (Olympus model BHT) and interfaced to an IBM-AT computer. The detector is a 512 channel diode array. The 514.5 nm line of the Coherent Innova 70 argon ion laser was used for excitation. The experimental details were as reported previously.¹

Results and Discussion

As reported in the previous paper crystals of diprotonated triethylenediamine triiodide grow from the site of laser illumination, and the solution phase contains DABCO- H_2^{2+} ion, perchlorate ion, and iodide ion. Figures 1 and 2 show the 625 to 1100 cm^{-1} region of the Raman spectra measured when the objective was focussed at distances corresponding to $0 \leq x \leq 400 \mu\text{m}$, for potentials of -200 and +200 mV respectively. Bands at 808 cm^{-1} (cage breathing mode of DABCO- H_2^{2+}) and 937 cm^{-1} (symmetric stretching mode of ClO_4^-) are apparent. The intensity of the latter band in both figures is low near the surface as expected and increases to a steady value. For -200 mV the 808 cm^{-1} intensity is largest near the silver surface but degrades as x increases. At this potential no crystals are present. For +200 mV, where crystals exist, the band intensity (marked b) of diprotonated DABCO ion is low when x is small, and a second peak (marked c) at 791 cm^{-1} is present when $x < 140 \mu\text{m}$. This band is characteristic of the crystals.

As discussed elsewhere in more detail⁵ the Raman intensity arises from a focal cylinder which depends on the objective lens used. In this case we used the Olympus MS Plan 50, ∞/o , $f =$

180, NA = 0.55 lens which collects information over a 29 μm region around the focal point. Thus even when the specimen is very flat, such as crystalline silicon, the depth profile shows width, Fig. 3A. Each point in this spectrum corresponds to a base-line corrected intensity from the silicon line near 520 cm^{-1} , measured at different distances x . The shape of Fig. 3A is independent of the Raman band used to obtain the plot, but rather is a property of the objective lens.

The true intensity $I^t(x)$ is related to the measured intensity, $I^m(x)$, by the convolution equation

$$I^m(x) = \int_{-\infty}^{\infty} I^t(x + \chi)W(\chi)d\chi$$

where W is a window function for the optical assembly.⁶⁻⁸

Because silicon has a flat surface, its spectrum can be used to estimate the window function for the lens used. Thus $W(\chi)$ is taken from the silicon distance profile. By deconvolution the true intensity can be reproduced. Fig. 3B results for the crystalline silicon sample. This profile still has a significant width. Thus the best spatial resolution Δx , that can be achieved is about 10 μm to-date.

In Fig. 4A the Raman intensity of the 937 cm^{-1} line of ClO_4^- is plotted versus distance from the electrode surface for the silver electrode at a cathodic potential of -200 mV. The deconvoluted intensities are shown in Fig. 5A. The intensities at negative distances (caused by the above convolution effect) are seen to be removed by deconvolution and the profile commences at $x \approx 0$ as expected. The corresponding plots for the diprotonated DABCO ion are shown in Figs. 4B and 5B. The Raman band of adsorbed iodide ion was also observed at this potential (not shown); Guzonas et al.⁴ have proposed the occurrence of $\text{DABCO-H}_2^{2+}\text{-Cl}_2^{2-}$ ion pairs or triplets on a silver electrode surface under comparable conditions. The specific adsorptivity of iodide is greater than that of chloride. Thus a similar situation may apply in this study and it is represented diagrammatically in Fig. 6 (-200 mV). This adsorbed iodide layer will affect the point of zero charge and will result in an accumulation of the DABCO-H_2^{2+} cations near the interface and in the

diffusion layer extending out some 200 μm from the electrode, judging from Fig. 5B. This provides a good explanation for the sharp and strong DABCO- H_2^{2+} peaks at negative potentials seen in Fig. 10 of ref. 1. On the other hand perchlorate anion experiences a repulsive force and its bulk concentration is apparently diminished for $0 < x < 150 \mu\text{m}$, judging from Fig. 5A, but is at its bulk value beyond this distance.

When the electrode potential is +200 mV, Figs. 7 and 8, the crystals of DABCO- $\text{H}_2^{2+} (\text{I}_3^-)_2$ are present on the electrode. The Raman intensities of ClO_4^- , DABCO- H_2^{2+} (808 cm^{-1}) and DABCO- $\text{H}_2^{2+}(\text{I}_3^-)_2$ (791 cm^{-1}) are presented in Fig. 7A, B, and C respectively. The corresponding deconvoluted concentration-distance profiles are shown in Fig. 8A, B, and C. The 808 cm^{-1} line has a constant intensity beyond 200 μm , indicating that this line arises from the bulk species as in Fig. 1, and 4B. The band at 791 cm^{-1} occurs for $x < 0.2 \text{ mm}$ and is assigned to DABCO- H_2^{2+} in the crystals. Fig. 8C suggests that the crystal packing is greatest at about 40 μm from the silver electrode and the crystals have actually grown to about 200 μm from the surface. This estimate is consistent with the microphotograph shown as Fig. 11 of ref. 1. Comparison of Figs. 8B and C reveals that the bulk DABCO- H_2^{2+} is in excess (above the bulk concentration value) just beyond the crystal surface at about 80 μm . Perchlorate concentration is also low near the crystals and is at its bulk value for $x > 200 \mu\text{m}$.

In Fig. 9 the concentration distance profile of the Raman peak at 150 cm^{-1} , ascribed to I_3^- ion, is shown. The shapes of the plots (Fig. 8C and 9B) are very similar. This supports the interpretation that the crystals contain I_3^- and DABCO- H_2^{2+} . Thus a picture unfolds which is summarized in Fig. 6B. The crystals have formed a dense array, maximizing at around 80 μm but extending out some 200 μm . The I_3^- has come from the surface iodide and is combining with the DABCO- H_2^{2+} in this crystal. The bulk DABCO- H_2^{2+} has a higher than average concentration just beyond the crystal at $\sim 100 \mu\text{m}$. The ClO_4^- concentration is steady beyond the crystal surface region.

The CDPRMS method has allowed us to map out a concentration-distance profile which seems intuitively reasonable. This approach to obtaining a spatial analysis of the interphase has potential for other such studies.

Acknowledgements

This work was supported by Grants from the Natural Sciences and Engineering Research Council of Canada, the Office of Naval Research (U.S.A.) and Grant-in-Aid No. 02854064 for Scientific Research from the Ministry of Education, Science and Culture of Japan.

References

1. Ozeki, T.; Irish, D.E. *J. Phys. Chem.* preceding paper.
2. Ozeki, T.; Irish, D.E. *J. Electroanal. Chem.* **1990**, 280, 451.
3. McCreery, R.L. *Progr. Analyt. Spectrosc.* **1988**, 11, 141.
4. Guzonas, D.A.; Irish, D.E.; Atkinson, G.F. *Langmuir* **1989**, 5, 787.
5. Ozeki, T.; Irish, D.E.; Odziemkowski, M. to be published.
6. Carley, A.F.; Joyner, R.W. *J. Electron Spectrosc. Relat. Phenom.* **1979**, 16, 1.
7. P.A. Jansson, Ed., *Deconvolution With Applications in Spectroscopy*, Academic Press, Inc.: Orlando, Florida, 1984.
8. Ozeki, T.; Watanabe, I.; Ikeda, S. *J. Electroanal. Chem.* **1983**, 152, 41.

Figure Captions

- Figure 1:** Raman spectra of the 650 to 1050 cm^{-1} region for the solution 0.5 M NaI, 0.1 M DABCO with pH 0.45, observed at the specified distances from the surface of a silver electrode polarized to -200 mV.
- Figure 2:** Raman spectra of the 650 to 1050 cm^{-1} region for the solution 0.5 M NaI, 0.1 M DABCO with pH 0.45, observed at the specified distances from the surface of a silver electrode polarized to +200 mV.
- Figure 3:** A: the peak intensity (520 cm^{-1}) - distance profile of a silicon crystal; B: the deconvoluted peak intensity-distance profile corresponding to the actual distribution of the silicon surface.
- Figure 4:** A: the peak intensity-distance profile for the perchlorate ion observed at 937 cm^{-1} ; B: that of the diprotonated DABCO ion at 808 cm^{-1} ; both were measured at -200 mV.
- Figure 5:** A: the deconvoluted peak intensity-distance profile of the perchlorate ion; B: that of the protonated DABCO ion; both were measured at -200 mV.
- Figure 6:** Schematic illustrations of the electrode/electrolyte interphase. A: at -200 mV; B: at +200 mV. Regions a, b, c, and d denote the silver metal, the interface between metal and solution, the solution side of the interphase, and the crystal formed upon the electrode, respectively.

Figure 7: A: the distance profile of the Raman intensity of the perchlorate ion observed at 937 cm^{-1} ; B: that of the band observed at 808 cm^{-1} of the diprotonated DABCO ion; C: that of the band observed at 791 cm^{-1} of the diprotonated DABCO ion, all measured at +200 mV.

Figure 8: The corresponding deconvoluted peak-intensity-distance profiles of A: the perchlorate ion; B: the diprotonated DABCO ion (808 cm^{-1}); C: the diprotonated DABCO ion in the crystal (791 cm^{-1}); all were measured at +200 mV.

Figure 9: A: the peak intensity-distance profile of the Raman band at 150 cm^{-1} ; B: its deconvoluted distance profile (corresponding to the concentration - distance profile of the total amount of I^- and I_3^-), measured at +200 mV.

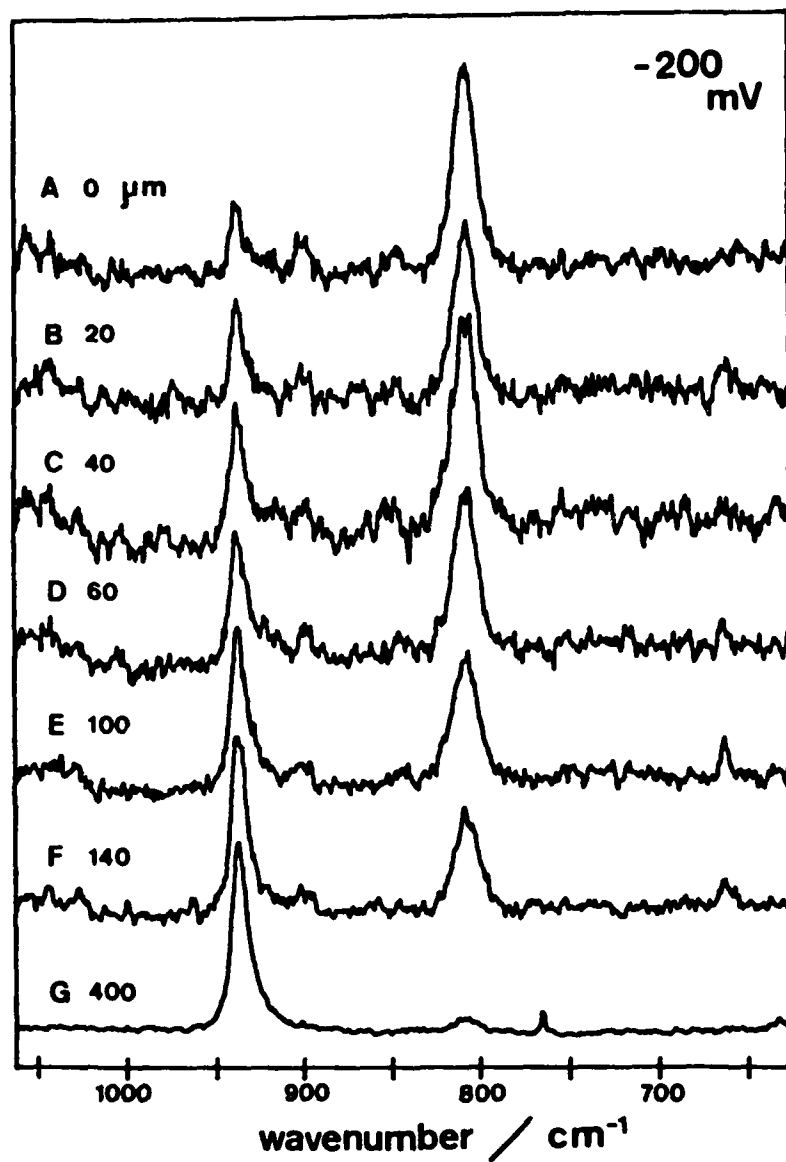


Figure 1: Raman spectra of the 650 to 1050 cm^{-1} region for the solution 0.5 M NaI, 0.1 M DABCO with pH 0.45, observed at the specified distances from the surface of a silver electrode polarized to -200 mV.

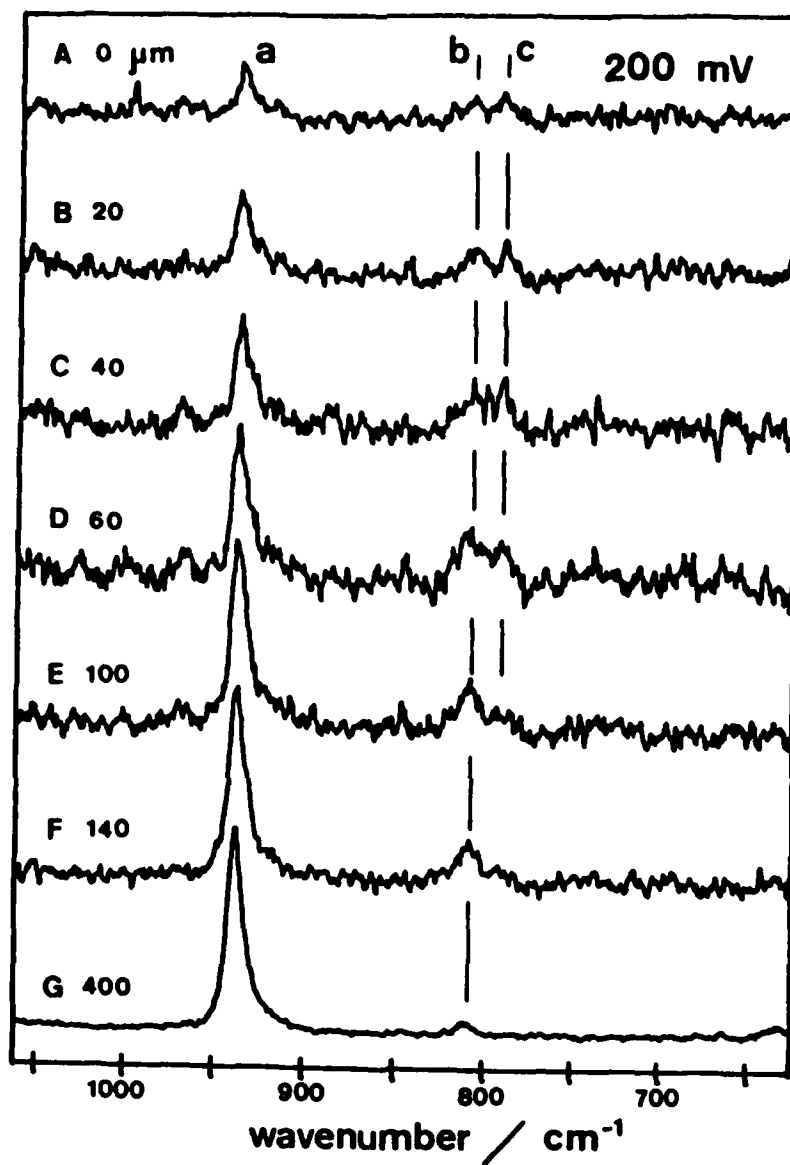


Figure 2: Raman spectra of the 650 to 1050 cm^{-1} region for the solution 0.5 M NaI, 0.1 M DABCO with pH 0.45, observed at the specified distances from the surface of a silver electrode polarized to +200 mV.

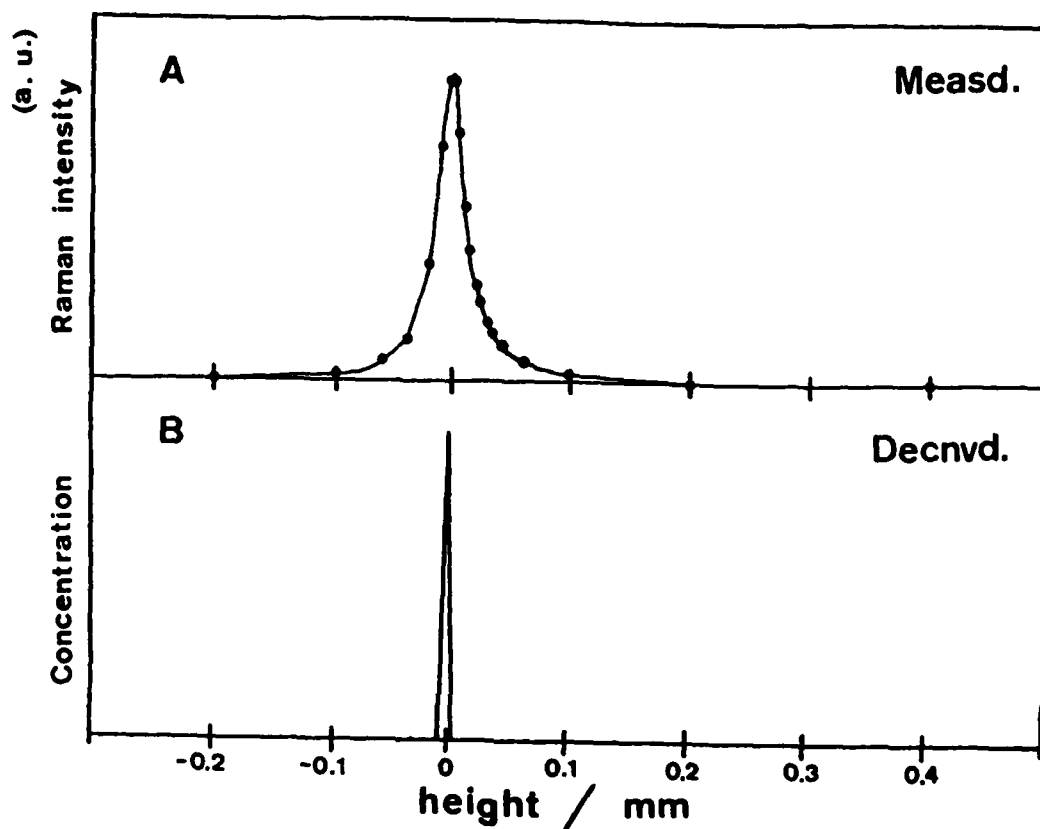


Figure 3: A: the peak intensity (520 cm^{-1}) - distance profile of a silicon crystal; B: the deconvoluted peak intensity-distance profile corresponding to the actual distribution of the silicon surface.

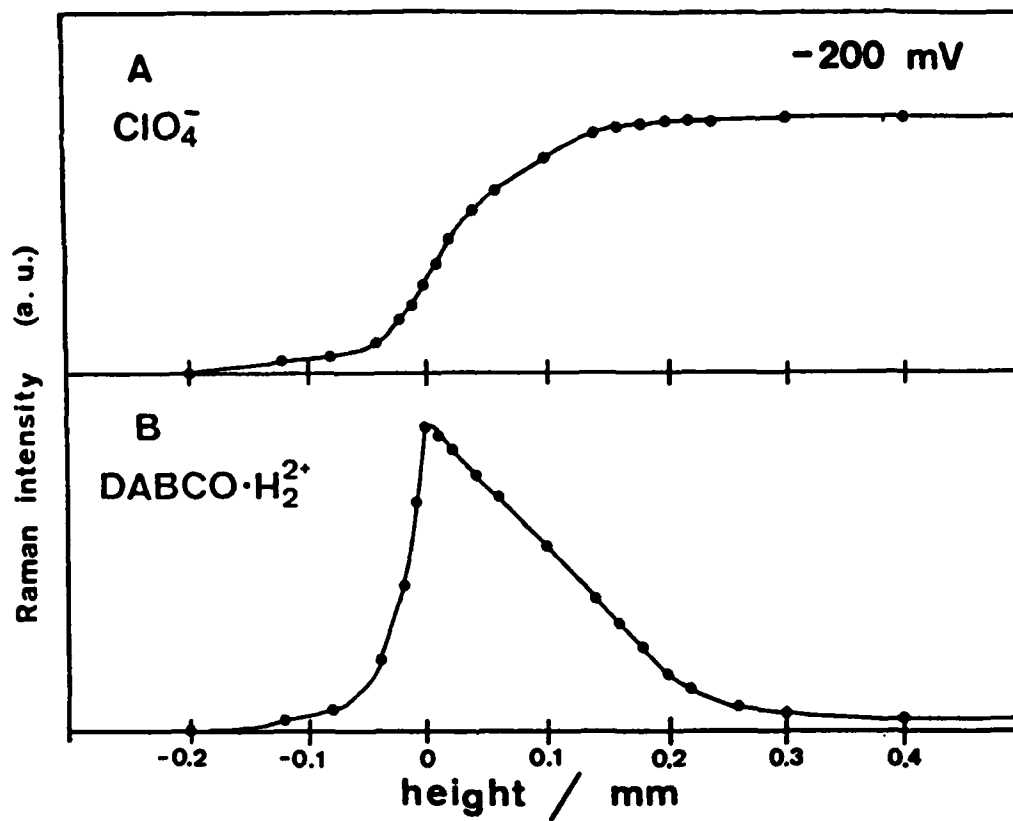


Figure 4: A: the peak intensity-distance profile for the perchlorate ion observed at 937 cm^{-1} ; B: that of the diprotonated DABCO ion at 808 cm^{-1} ; both were measured at -200 mV .

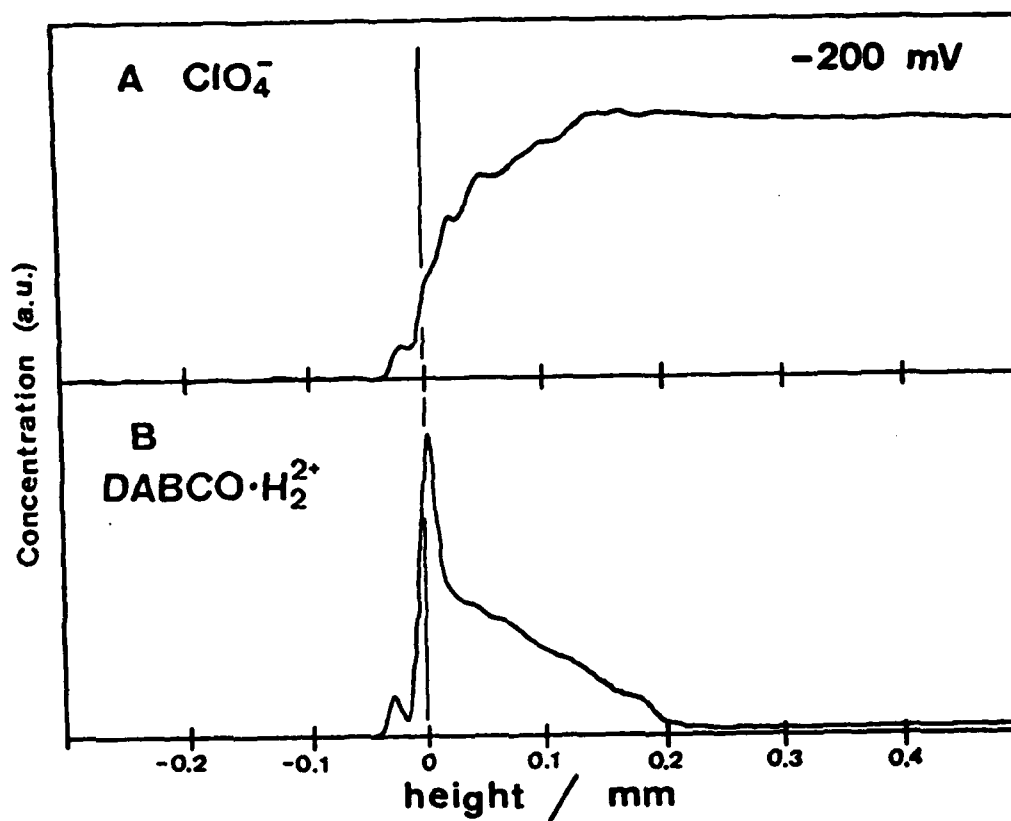


Figure 5: A: the deconvoluted peak intensity-distance profile of the perchlorate ion; B: that of the protonated DABCO ion; both were measured at -200 mV.

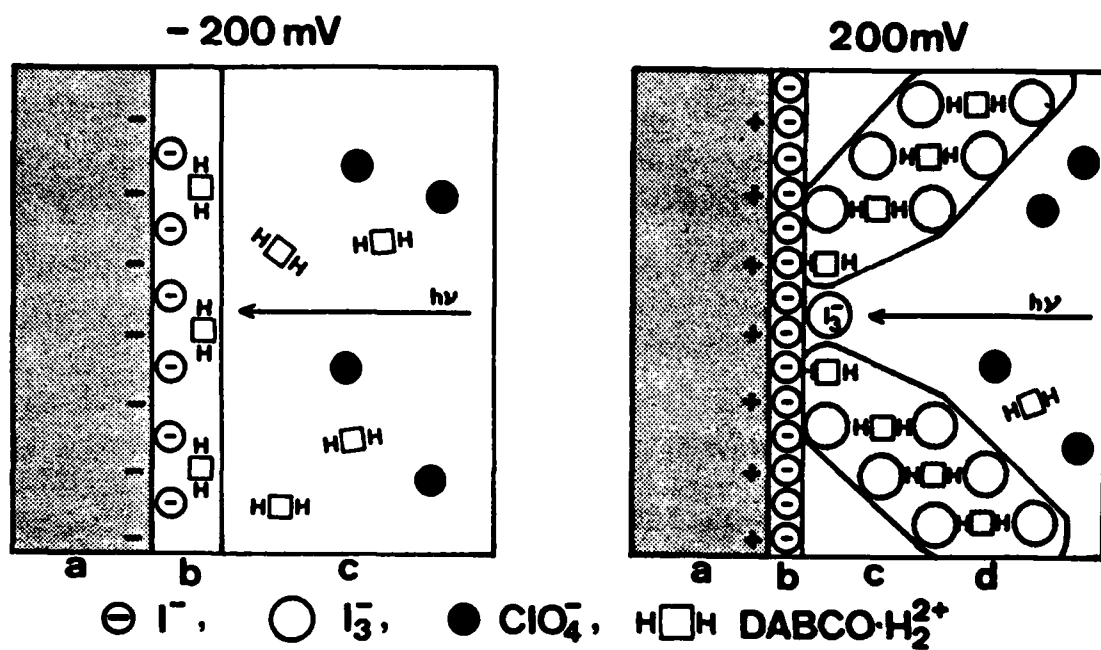


Figure 6: Schematic illustrations of the electrode/electrolyte interphase. A: at -200 mV; B: at +200 mV. Regions a, b, c, and d denote the silver metal, the interface between metal and solution, the solution side of the interphase, and the crystal formed upon the electrode, respectively.

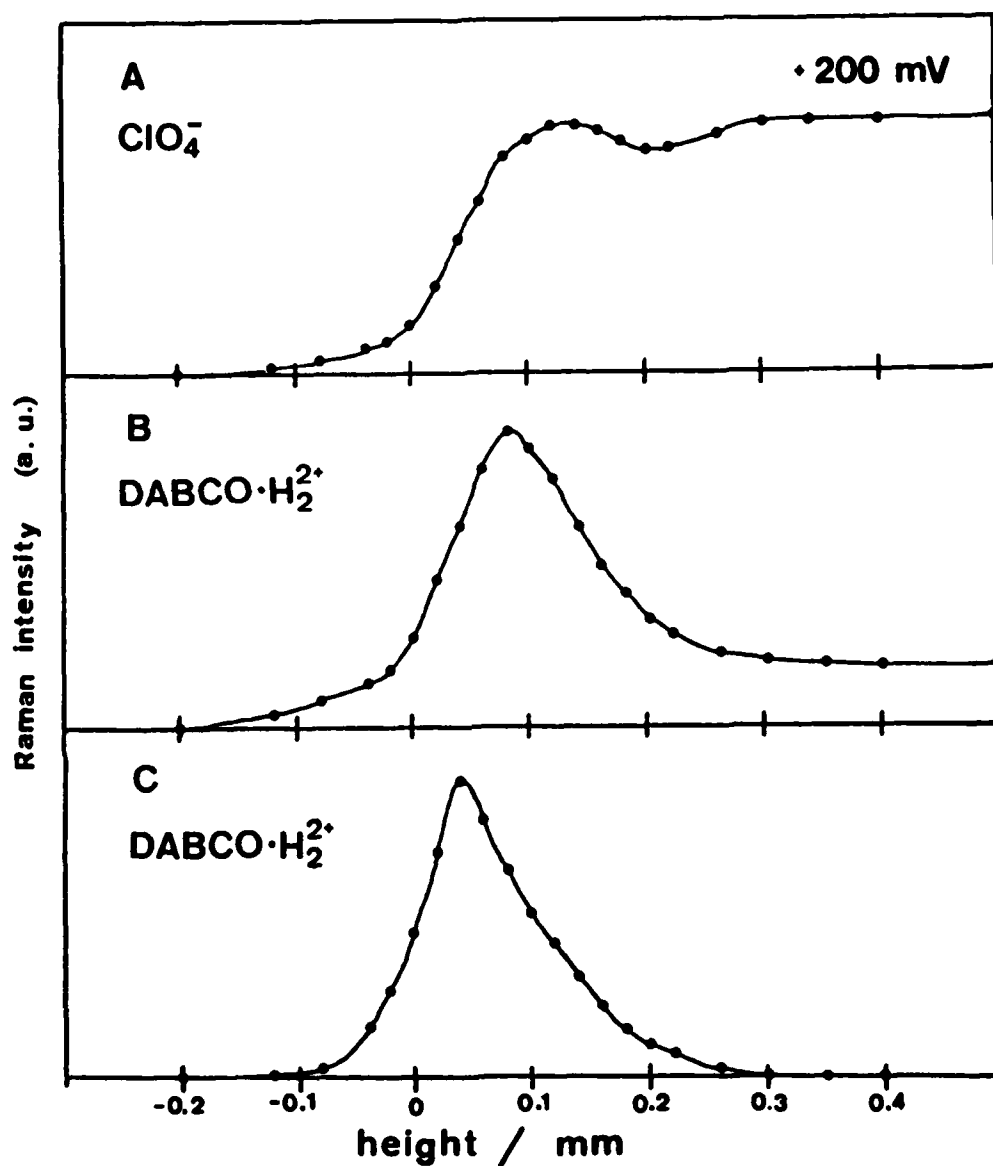


Figure 7: A: the distance profile of the Raman intensity of the perchlorate ion observed at 937 cm^{-1} ; B: that of the band observed at 808 cm^{-1} of the diprotonated DABCO ion; C: that of the band observed at 791 cm^{-1} of the diprotonated DABCO ion, all measured at +200 mV.

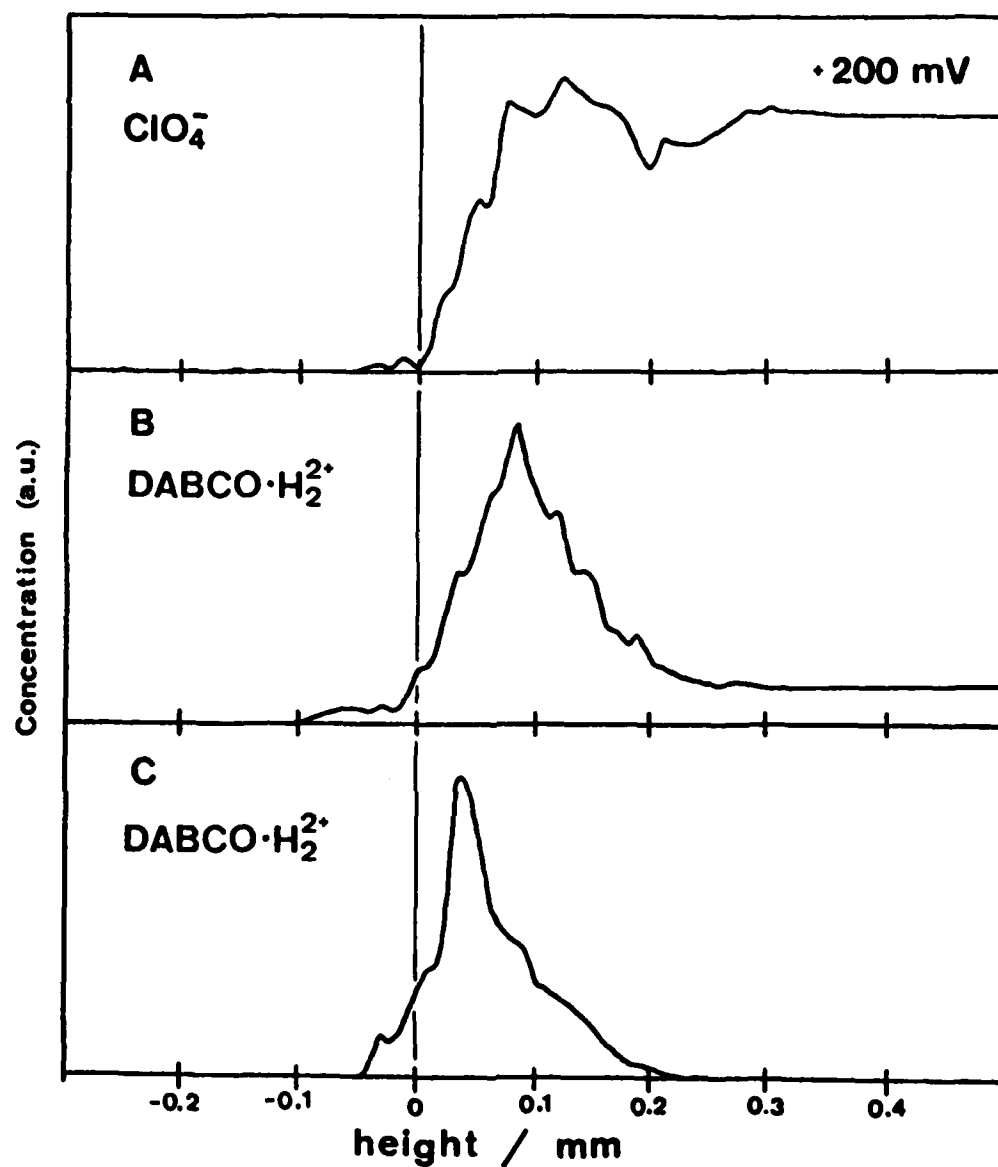


Figure 8: The corresponding deconvoluted peak-intensity-distance profiles of A: the perchlorate ion; B: the diprotonated DABCO ion (808 cm^{-1}); C: the diprotonated DABCO ion in the crystal (791 cm^{-1}); all were measured at +200 mV.

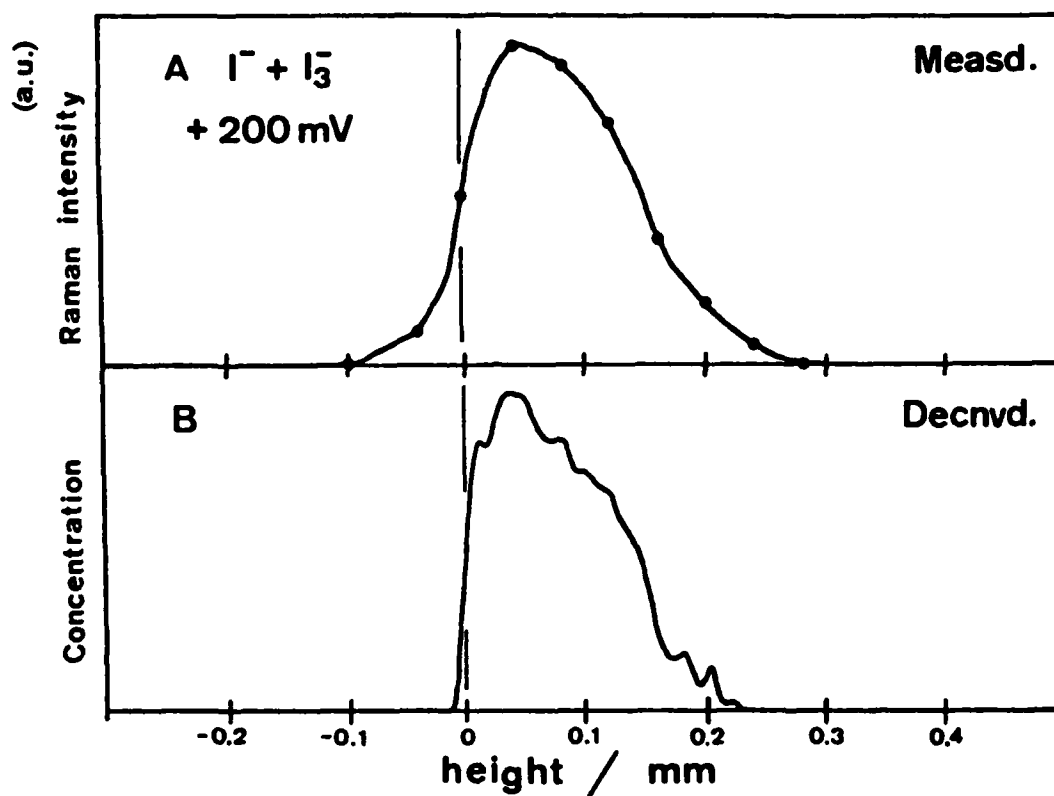


Figure 9: A: the peak intensity-distance profile of the Raman band at 150 cm^{-1} ; B: its deconvoluted distance profile (corresponding to the concentration - distance profile of the total amount of I^- and I_3^-), measured at +200 mV.

TECHNICAL REPORT DISTRIBUTION LIST - GENERAL

Office of Naval Research (2)
Chemistry Division, Code 1113
800 North Quincy Street
Arlington, Virginia 22217-5000

Commanding Officer (1)
Naval Weapons Support Center
Dr. Bernard E. Douda
Crane, Indiana 47522-5050

Dr. Richard W. Drisko (1)
Naval Civil Engineering
Laboratory
Code L52
Port Hueneme, CA 93043

David Taylor Research Center (1)
Dr. Eugene C. Fischer
Annapolis, MD 21402-5067

Dr. James S. Murday (1)
Chemistry Division, Code 6100
Naval Research Laboratory
Washington, D.C. 20375-5000

Defence Technical Information (2)
Center
Building 5
Cameron Station
Alexandria, VA
U.S.A. 22314

Dr. Robert Green, Director (1)
Chemistry Division, Code 385
Naval Weapons Center
China Lake, CA 93555-6001

Chief of Naval Research (1)
Special Assistant for Marine
Corps Matters
Code 00MC
800 North Quincy Street
Arlington, VA 22217-5000

Dr. Bernadette Eichinger (1)
Naval Ship Systems Engineering
Station
Code 053
Philadelphia Naval Base
Philadelphia, PA 19112

Dr. Sachio Yamamoto (1)
Naval Ocean Systems Center
Code 52
San Diego, CA 92152-5000

Dr. Harold H. Singerman (1)
David Taylor Research Center
Code 283
Annapolis, MD 21402-5067

ENCLOSURE(2)